Paramagnetic centers and dipolar defects in CaF_2:Gd^{3+} and CaF_2:Gd^{3+}+Lu^{3+}

E. Laredo, M. Díaz, N. Suarez, and A. Bello
Department of Physics, Universidad Simón Bolívar, Apartado 89000, Caracas 1080, Venezuela
(Received 10 April 1992)

The combined results obtained on $Ca_{1-x}Gd_xF_{2+x}$ and $Ca_{1-x-y}Lu_xGd_yF_{2+x+y}$ solid solutions by ionic thermal currents and electron paramagnetic resonance techniques are presented for a wide range of x values. The Gd^{3+} ions are located in tetragonal and cubic sites, and in a variety of at least nine polarizable entities in the single-doped solid solutions whose range of existence and relaxation parameters have been precisely determined. In the double-doped crystals the Gd^{3+} probes are in constant concentration (y=0.0001) while the Lu^{3+} ions detected in the temperature range explored here constitute a very small fraction of the nominal concentration of the sample. The differences observed are accounted for by a scavenging of F_i^- by clusters of increasing size in the single-doped matrix and by the existence of cubo-octahedra hexamers existing from very low doping levels in the double-doped crystals.

I. INTRODUCTION

The fluorite matrices doped with trivalent cations have been extensively studied in the last decade. The interest in these crystals is due to their ability to accommodate large molar fractions of trivalent impurities that form solid solutions within the fluorite structure until nearly 50% of the alkaline earth ions are replaced. No incoherent precipitates have been detected. The x-ray diffraction patterns for the intermediate concentration range only show a distortion of the lattice whose sign and magnitude vary as a function of the ratio of the cationic radii of the dopant to that of the host matrix. In the high concentration range superstructures based on cubo-octahedra clusters have been proposed after the x-ray diffraction studies of Bevan, Strahle, and Greis.[1] Even if the average crystal structure of the host matrix is preserved, the introduction of impurities locally creates zones where the symmetry is much lower than that of the overall structure. The perfect fluorite structure is visualized as an assembly of small cubes of fluoride ions, with a periodicity equal to half the lattice parameter of the fluorite unit cell, whose centers are alternatively occupied by the divalent cations. On doping, the trivalent cation R^{3+} is located in the center of a cube of F^- ions in substitution of the divalent cation; the charge compensating defect occupies one of the centers of the fluorine cubes which is normally empty in the perfect lattice, creating an interstitial fluorine, F_i^-. One can then imagine the whole variety of situations that can occur depending on the number and relative positions of these two point defects. The closest positions originate a monomer with a dipolar moment that is the nearest-neighbor (NN) dipole whose point symmetry is tetragonal, C_{4v}, while the next-nearest neighbor (NNN) dipole parallel to one of the cube main diagonals has a trigonal symmetry. If the F_i^- is farther apart from the R^{3+}, then the free cation will be in a cubic environment due to the nonlocal compensation.

At higher concentrations the probability of forming clusters of these simple defects increases, and dimers, trimers, and tetramers are probable. Theoretical calculations using the standard computer simulation procedure HADES,[2,3] based on the well-known Mott and Littleton model, have shown that in CaF_2:R^{3+} clustering increases the stability of the lattice. These estimates for the whole lanthanide series and Y^{3+}, show a definite tendency towards the aggregation of simple defects and the trapping of extra interstitial fluorines by these clusters. Various experimental techniques have been used to study these systems and in the case of the $Ca_{1-x}R_xF_{2+x}$ solid solutions the most studied impurities have been Er, Pr, and Gd. Ionic thermal current (ITC) experiments have been performed[4] on gadolinium-doped CaF_2 ($0.0001 \leq x \leq 0.01$) and two main dipolar defects have been found in this low and intermediate concentration range. The first one (T_M=131 K) was attributed to the disorientation of NN dipoles, which is the predominant specie for $x \leq 0.001$. The second one, located 90 K higher, was less intense and its intensity peaked at $x = 0.002$. The comparison of the behavior of these two peaks after quenching from high temperatures leads Capelletti *et al.*[4] to assign the second relaxation to a cluster of dipoles that might have trapped an extra F_i^-. In the case of lanthanum-doped CaF_2 crystals in the same concentration range we have found[5] that the number of NN dipoles decreases as x grows and that they form a very small fraction of the nominal La^{3+} concentration of the crystal. Dielectric relaxation techniques have also been used to study the dipolar defects in CaF_2. Andeen *et al.*[6] studied the dielectric constant of CaF_2 doped with 1% of 13 rare earths. They found that at this impurity concentration the dominant relaxation is located at very low temperatures from Tb to Lu and that it is either associated with a higher-order complex or a superstucture. For the largest rare-earth cations (Ce to Gd) the gettered dimer relaxation dominates the spectrum. The ITC technique is sensitive and precise, but it cannot by itself provide information on the exact structure of the

dipolar specie that is causing the observed peaks; furthermore, all the impurities that are not in polarizable entities, whether the resulting dipolar moment is null or a reorientation path does not exist, will not show in the resulting ITC or dielectric constant spectrum. Spectroscopic techniques such as electron paramagnetic resonance (EPR), site selective laser excitation, and optical absorption are then necessary if one wants to achieve a better understanding of the structure of each of the various species that obviously coexist in these matrices. Very diluted CaF_2:Gd^{3+} crystals have been extensively studied by EPR, and cubic and tetragonal sites were found. In reviewing the early articles one notices that these pioneer works showed a certain amount of discrepancy on the number of different crystal-field splittings found and on the relative abundance of each of these centers. Friedman and Low[7] reported how a quenching from high temperature or an annealing followed by slow cooling could affect the relative abundances of the cubic and tetragonal Gd^{3+} spectra. The cubic and tetragonal spectra at these very low concentrations have been attributed to the free Gd^{3+} substitutional ions in equilibrium with the NN Gd^{3+}-F_i^- dipoles. Several authors[8] reported at that time the existence of trigonal centers that were due to the charge compensation of Gd^{3+} by substitutional O^{2-} ions present in oxygen contaminated crystals. Later on, when the charge compensating mechanism originating the simple NN and NNN dipoles was well established, a careful search[9] for the trigonal NNN dipole easily observed in BaF_2 and SrF_2, gave null results in CaF_2. The influence on the site symmetry of the introduction of monovalent ions (Na, K, and Ag) on the Gd^{3+} cubic and tetragonal centers was also quantitatively investigated[10] and it was shown that the abundance of cubic centers increased as the Na^+ content grew; simultaneously the tetragonal centers slowly disappeared.

Site selective laser spectroscopy has been widely used recently to characterize the different sites occupied by praseodymium[11,12] and erbium[13–15] in CaF_2. The conclusion is that even at the very low concentrations used in these works trivalent cations exist as dimers. Also the existence of higher-order clusters is demonstrated in both cases. Tallant, Moore, and Wright[14] determined the absolute site concentrations as a function of the erbium molar concentration ($10^{-6} \leq x \leq 10^{-2}$) showing a definite maximum in the number of tetragonal sites around $x = 10^{-3}$ while most of the sites associated with clusters are still growing in number at these concentrations.

The number of cubic centers and its variation with x have also deserved a considerable amount of discussion and speculation about their origin and how such a high concentration can coexist with the other types of defects. Recently, Moore and Wright[15] have shown that the number of cubic centers is an increasing function of the Er ion molar fraction, and they precisely determined the site distribution in the dilute and intermediate concentration range ($x \leq 0.002$). The previous explanations advanced in earlier works, to account for this unexpected abundance of cubic centers observed by EPR techniques, were commented on by Secemski and Low.[16] The difficulties of accepting the existence of a local cubic phase[17] RF_3:$3CaF_2$ without observing any changes in the x-ray diffraction pattern of these solid solutions, or to the spatial averaging of a dimer of simple dipoles whose symmetry is C_{2v} were stressed. Secemski and Low[16] then proposed that the equilibrium temperature of the fluorite samples should be higher than the accepted value of about 630 K. Tallant, Moore, and Wright[14] proposed a model based on the existence of two different equilibria. The trivalent cation site distribution is frozen at a high temperature while the F_i^- ions are still mobile; these fluoride ions reach equilibrium at a much lower temperature, thus allowing a gettering process by the fixed cations in the lattice. This process would result in an excess number of F_i^- around the clustered pairs and in a high concentration of nonlocally compensated trivalent cations caused by the scavenging of the F_i^- by the higher clusters than the NN or NNN dipoles. This model has been reviewed by Moore and Wright[15] and even if it explains most of the site distribution observed as a function of the dopant concentration, it does not explain the concentration dependence when applied to crystals quenched from high temperature where it is assumed that the clusters are dissociated.

In this work we present the results obtained on the $Ca_{1-x}Gd_xF_{2+x}$ solid solutions in a wide x range ($0.0001 \leq x \leq 0.1$) with ionic thermal currents and electron paramagnetic resonance techniques. The same studies were performed on double-doped crystals $Ca_{1-x-y}Lu_xGd_yF_{2+x+y}$ with a fixed amount of Gd ($y = 10^{-4}$) and a variable concentration of Lu ($0.0001 \leq x \leq 0.02$). The two experimental techniques are complementary as the first one is sensitive to dipolar defects such as the NN, NNN, and any polarizable cluster that can reorient in an external electric field, while the second will give us information about the symmetry of the crystalline field as seen by the different paramagnetic centers. The absolute concentration of dipoles can be calculated from the area or the height[18] of each relaxation peak if the dipolar moment μ is known. Both techniques can follow the relative abundances of each type of defect. The comparison of the results obtained in a very wide concentration range on both the single- and double-doped crystals should help to complete the detailed picture that has been drawn by previous authors for Er and Pr. Also, Gd, being midway in the series between Er and Pr, is a good choice to clarify if there is any size effect in the site distribution of trivalent ions in CaF_2. We will show the existence of at least nine different relaxation processes and follow the intensity of the identified paramagnetic centers in order to compare the information provided by the two methods. Also the use of the Gd ions as paramagnetic probes in the case of the double-doped crystals will help in reaching a conclusion on the clustering effect of the smallest of the rare-earth ions.

II. EXPERIMENT

The samples used in this work were single crystals purchased from Optovac, Inc. The nominal molar fractions for the single-doped samples ranged from 2×10^{-7} to 10^{-1} and we have found that they are in good rela-

tion to the total Gd^{3+} content. The crystalline quality of the Gd doped samples allowed us to cleave them easily along {111} faces except for the three highest concentrations. The double-doped crystals were difficult to cleave as the boule presented tensions even from the lowest Lu concentration studied here. The solid solutions $Ca_{1-x-y}Lu_xGd_yF_{2+x+y}$ were studied in an x range from 0.0001 to 0.02, with a fixed value for $y = 0.0001$. The EPR experiments were carried out at room temperature in a Varian E-line spectrometer working in the X-band ($\nu = 9.51$ GHz), with a TE_{110} cylindrical cavity. A Sentec NMR magnetometer was used to measure the magnetic field H_0, with a precision of 0.02 G, together with a Hewlett-Packard frequency counter that read the microwave frequency to better than 1 ppm. A data acquisition system consisting of a Hewlett-Packard digital voltmeter and scanner, and an IBM-AT personal computer as the controller, was interfaced with the spectrometer to record the data for further analysis. The crystals were cleaved along four {111} planes with an average size of $2 \times 2 \times 8$ mm^3. They were mounted on sample rods with a [110] axis vertical in order to have H_0 parallel to a (110) plane where the three principal crystallographic directions lie.

The ionic thermal currents were carried in a setup that has previously been described.[18] The samples were disk-shaped crystals with {111} faces with an area of 1 cm^2 and about 1 mm thick. The system had a sensitivity better than 5×10^{-16} A. Three different types of ITC runs were performed on each sample. First, the crystal was polarized at room temperature and the spectrum was recorded in order to identify the various current peaks present from 77 to 300 K; then a polarization temperature near the temperature of each current maximum, T_M, was chosen and a subsequent run was performed in order to minimize the influence of the higher-temperature peaks. The intensities of the different relaxations were measured from these spectra. Then each peak was again polarized near the temperature of the current maximum, the crystal quenched rapidly to 77 K, the field switched off, the temperature rose to the vicinity of T_M and it was cooled again in order to clean the peak from all contributions of relaxations located at lower temperatures. These clean peaks were used to determine the relaxation times τ for the different processes present in the matrix by fitting the ITC peaks with the procedure proposed by us[19] which allows the reorientation energy to be either single valued or distributed around a mean value E_0.

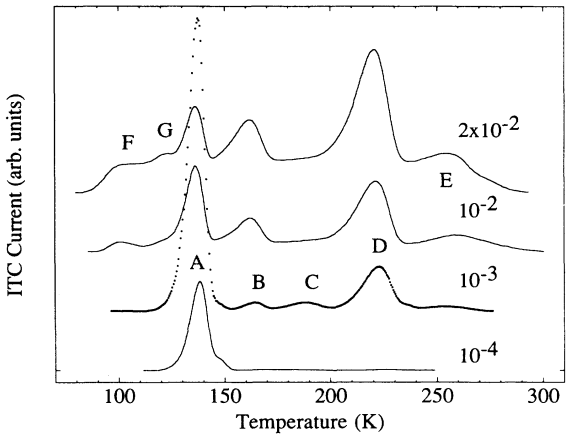

FIG. 1. ITC spectra of the $Ca_{1-x}Gd_xF_{2+x}$ solid solutions for different x values.

III. RESULTS

A. $Ca_{1-x}Gd_xF_{2+x}$ solid solutions

1. ITC experiments

For the lowest x values the ITC spectrum consists of a single relaxation peak with its maximum at T_{MA}=138 K. The spectrum becomes increasingly complicated as x starts growing due to the appearance of six new peaks. Peaks B, C, D, and E are at higher temperatures than peak A while peaks F and G are at lower temperatures as can be seen in Fig. 1. The variation of the intensity of the A peak versus x is the only one that shows a maximum for $x = 10^{-3}$. The intensity of the other six peaks steadily increases with the doping level and becomes very rapidly predominant after 1% as shown in Fig. 2. Table I shows the results of the fittings performed on efficiently cleaned ITC peaks for the relaxation parameters, allowing a Gaussian distribution of the reorientation energy characterized by a mean value E_0 and a width σ. These values were determined in the samples where the peak under study could be best isolated by the usual peak-cleaning procedures that minimize the influence of nearby overlapping peaks. It should be noted that the reorientation energy is single-valued for the NN relaxation (peak

TABLE I. Best-fit relaxation parameters for the $Ca_{1-x}Gd_xF_{2+x}$ solid solutions.

	x (Molar fraction)	T_M (K)	E_0 (eV)	σ (eV)	τ_0 (s)
Peak A	0.0001	138	0.439	0	3.1×10^{-15}
	0.001	138	0.421	0	1.3×10^{-14}
	0.01	138	0.419	0	1.2×10^{-14}
Peak B	0.01	163	0.481	9.5×10^{-3}	8.0×10^{-14}
Peak C	0.001	188	0.621	1.3×10^{-2}	1.3×10^{-15}
Peak D	0.01	221	0.636	0	2.2×10^{-13}
Peak F	0.01	101	0.166	6.7×10^{-3}	3.2×10^{-7}
Peak G	0.02	124	0.359	1.0×10^{-2}	6.8×10^{-14}

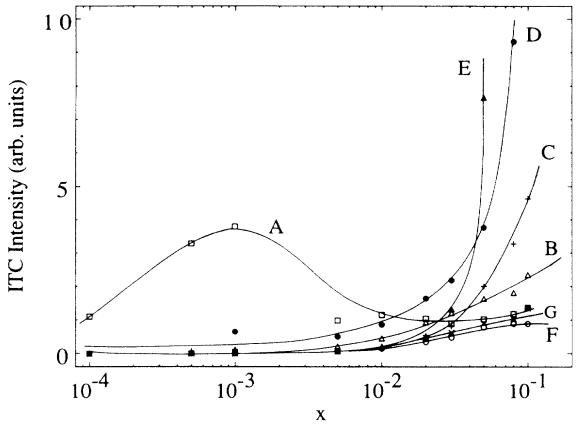

FIG. 2. Variation of the intensity of seven ITC peaks vs x in $Ca_{1-x}Gd_xF_{2+x}$ solid solutions. □: peak A, T_{MA}=138 K; △: peak B, T_{MB}= 163 K; +: peak C, T_{MC}= 189 K; ●: peak D, T_{MD}= 221 K; ▲: peak E, T_{ME}= 260 K; ○: peak F, T_{MF}= 101 K; ×: peak G, T_{MG}= 124 K. The lines are drawn to guide the eye.

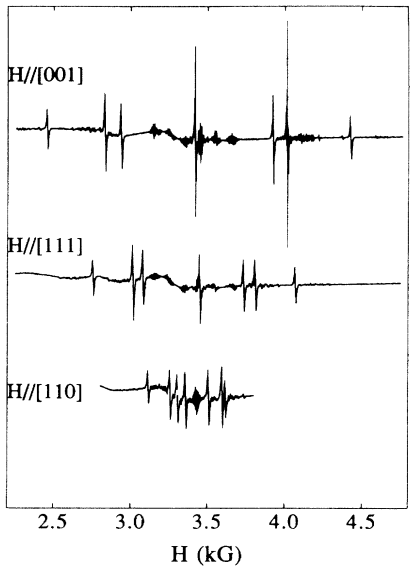

FIG. 3. Room-temperature EPR spectra of 2×10^{-7} Gd^{3+} in the CaF_2 single-doped crystal for three directions of the external field.

A), and for the most intense peak (peak D), even for the most highly doped samples. The other peaks could only be properly fitted if a Gaussian distribution in the activation energy was taken into account. The reported values for σ are large for concentrations as low as 0.001, showing that a variation of the energy barriers is either somewhat different due to lattice strains, or the ion jumps are not identical and there exist several reorientation paths that differ slightly in energy. Moreover, the peak labeled E which corresponds to the highest-temperature relaxation was fitted only after it was decomposed into three peaks located at 257, 273, and 289 K whose respective energies are 0.676 and 0.711 eV, the third one being too weak to be properly adjusted. In brief, we have been able to detect and characterize nine different current peaks in the ITC spectra of the $Ca_{1-x}Gd_xF_{2+x}$ crystals, showing the complexity of the equilibrium among all the species coexisting in the matrix.

2. *EPR experiments*

The very dilute Gd^{3+} doped crystal, $x = 2\times10^{-7}$, gave the spectra presented in Fig. 3 when H_0 was parallel to the [001], [111], and [110] directions. These spectra correspond to a Gd^{3+} ($^8S_{7/2}$) in a cubic site with the typical seven-line spectrum whose positions vary with the orientation of the external field as shown in Fig. 4. The spin Hamiltonian parameters b_ℓ^m were fitted by using a Monte Carlo computing procedure that has been described in detail elsewhere.[20] The solid lines drawn in Fig. 4 are the result of the calculation of the positions of the seven cubic lines as a function of the relative orientation of the sample and H_0 based on the set of parameters found by the Monte Carlo method. The good agreement among the calculated and the experimental positions shows that the values of the crystal-field parameters found here are most reliable and precise.

The crystal with the lowest concentration studied here was so diluted that we were also able to resolve at room temperature the superhyperfine splitting of several of the fine-structure cubic lines. A second Monte Carlo procedure described elsewhere[21] was written to adjust the tensor components of the superhyperfine Hamiltonian in order to best fit the observed intensity of the fine structure lines that are the envelope of the numerous lines assumed to be due to the interaction among the electronic spin of

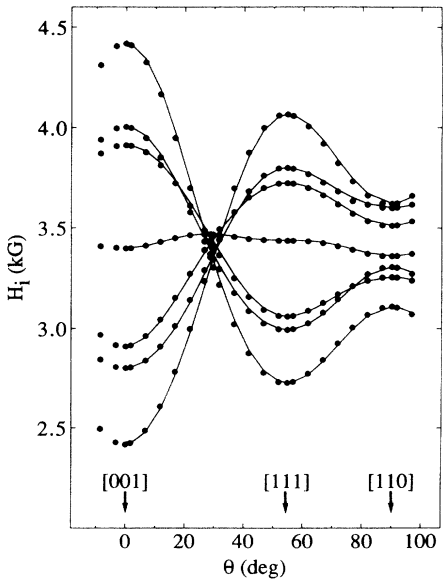

FIG. 4. Angular dependence of the seven line cubic spectra of Gd^{3+} in CaF_2 crystals. The lines result from the calculation of the spectrum with the spin Hamiltonian parameters determined with the Monte Carlo fitting procedure.

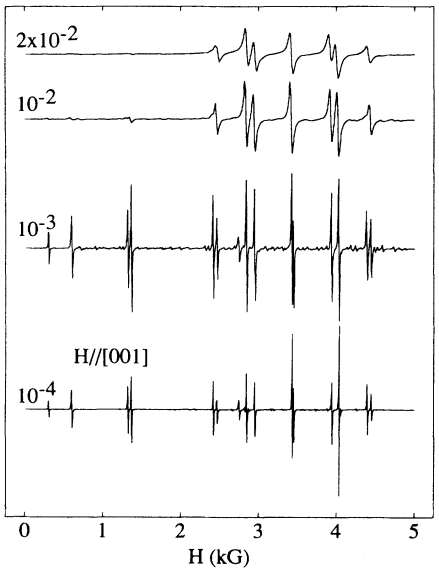

FIG. 5. Room-temperature EPR spectra of the $Ca_{1-x}Gd_xF_{2+x}$ solid solutions as a function of x for the H|| [001] direction.

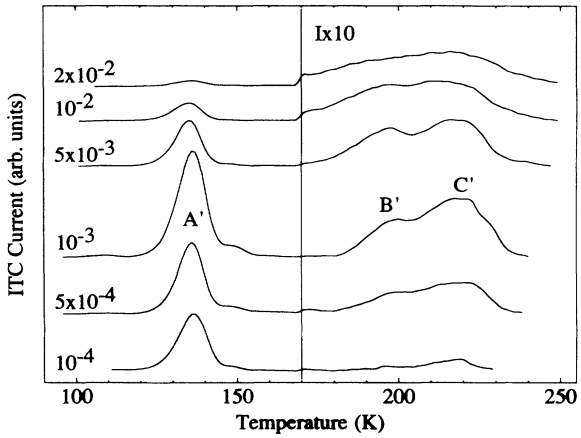

FIG. 6. ITC spectra of the $Ca_{1-x-y}Lu_xGd_yF_{2+x+y}$ solid solutions for different x values and $y = 0.0001$.

the Gd located at the center of a fluorine cube and the nuclear spins of the eight equidistant neighboring anions. The agreement between the calculated curve and the experimental one was excellent and the model for the structure of this center of a simple substitutional Gd^{3+} in the center of a fluorine cube was thus confirmed. The intensity of the cubic spectrum was found to be predominant at high concentrations in the single-doped matrix as can be observed in Fig. 5. This intensity is a steep increasing function with x. The fine structure splitting does not present any change in the whole concentration range studied here; only a line broadening was observed due to the spin-spin interaction, but no change in the crystal-field parameters was found for this broadened spectrum as compared to those determined for the very dilute system. Thus, one can state that the cubic center does not undergo either a structural variation or a change in its origin over the whole concentration range surveyed in this work.

For the second concentration studied here, $x = 0.0001$, a second spectrum is present with an intensity comparable to that of the cubic spectrum at this Gd^{3+} concentration. The new spectrum was fitted with a spin Hamiltonian corresponding to a C_{4v} local symmetry.[20] The intensity variation of the tetragonal center spectrum vs x, shows a peak for $x = 0.001$ and then starts decreasing. For the highest concentration, as for the most dilute crystal, the cubic center is the only one detected.

B. $Ca_{1-x-y}Lu_xGd_yF_{2+x+y}$ solid solutions

1. *ITC experiments*

The ITC spectrum as the Lu molar fraction increases, shown in Fig. 6, is simpler than before. It consists of one main relaxation, A', located at 138 K; as the x value increases there appears two broad and very weak relaxations around 200 and 220 K. The variation of each peak intensity with the concentration of Lu^{3+} ions is represented in Fig. 7. The intensity variation is here totally different as compared to the single-doped samples as, at high Lu^{3+} concentrations, there is no evidence of the existence of polarizable complexes besides those already present at low x values. The most intense peak of the spectrum, A', occurs at the same temperature as the A peak of the Gd^{3+} doped crystals but it is much weaker. The intensities of the other two relaxations observed here also show a maximum around $x = 3\times10^{-3}$, although they are about 30 times less intense than that of peak A' as shown in Fig. 7.

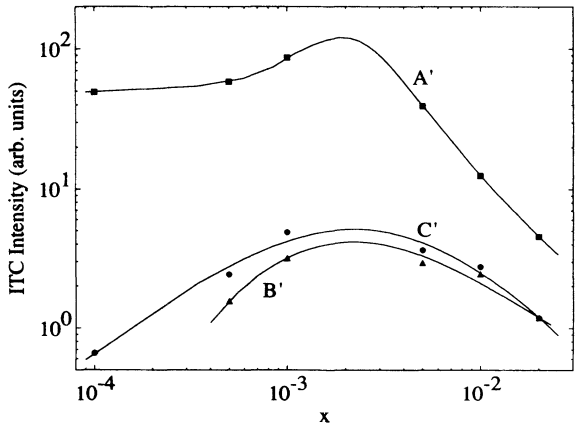

FIG. 7. Variation of the intensity of the ITC spectrum vs x ($y = 0.0001$) in solid solutions of $Ca_{1-x-y}Lu_xGd_yF_{2+x+y}$. ■: peak A', $T_{MA'}$=137 K; ▲: peak B', $T_{MB'}$= 199 K; •: peak C', $T_{MC'}$= 220 K. The lines are drawn to guide the eye.

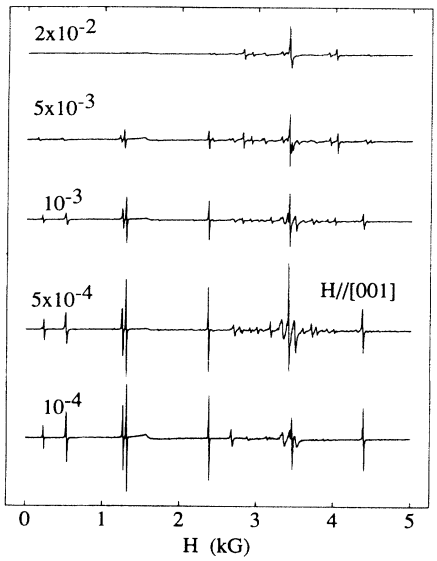

FIG. 8. Room-temperature EPR spectra of the $Ca_{1-x-y}Lu_xGd_yF_{2+x+y}$ solid solutions as a function of x for the H|| [001] direction.

2. *EPR experiments*

The room-temperature EPR spectrum as the Lu^{3+} concentration varies is very simple and composed of cubic and tetragonal Gd^{3+} centers in proportions that vary with x. The spin Hamiltonian parameters found by using the simulated thermal annealing are identical to those determined for the single-doped Gd^{3+} crystals. The EPR spectra given by the Gd^{3+} in these double-doped crystals ($y = 0.0001$) are shown in Fig. 8. The cubic Gd^{3+} spectrum is not present in the sample with $x = 0.0001$, as it is in the case of the single-doped crystal with the same amount of Gd^{3+}; only the tetragonal center is detected. When x grows, the number of Gd^{3+} cubic centers starts to increase while the number of tetragonal defects slowly and continuously decreases. These cubic centers for $x \geq 0.01$ decrease in number but they remain the predominant Gd^{3+} paramagnetic centers for the highest Lu^{3+} concentrations. If one adds up the concentration of Gd^{3+} ions in cubic and tetragonal sites it is found that this sum is a slowly decreasing function of the Lu content of these crystals. The total Gd^{3+} concentration detected by EPR is at the utmost one-fifth of the 0.0001 nominal molar fraction.

IV. DISCUSSION

A. Tetragonal centers

The tetragonal Gd^{3+} centers identified in both solid solutions must correspond to a simple defect as their absence for the highest doping levels indicates that higher clusters are forming by their aggregation. The tetragonal center is attributed to the NN Gd^{3+}-F_i^- dipole that should also be detected by ITC techniques. The A peak in the single-doped matrix presents an intensity variation vs x identical to that observed for the tetragonal site. If one assumes that we are detecting the same specie the absolute concentrations of the Gd^{3+} centers can be calculated from the area under the curve of the ITC peak. Then, by normalizing the EPR intensity for one Gd^{3+} concentration, the variation of the concentration of NN dipoles determined from both methods can be compared; Fig. 9 represents both results. The agreement in the low concentration range is excellent. At high concentrations there is a small discrepancy, the ITC determination of the concentration of NN Gd^{3+} dipoles being systematically higher than that determined by EPR. The reason for this overestimation is due to the more intense high-temperature peaks that somewhat overlap the A peak and make the determination less precise at high concentrations where these peaks are predominant. From this figure one can also note the small fraction of the total Gd^{3+} concentration forming NN dipoles, thus indicating that most of the Gd^{3+} ions are in other sites. Furthermore, the existence of at least six ITC peaks in addition to the NN peak also shows the progressive formation of polarizable clusters whose existence will be discussed later on.

In the double-doped crystals, as it has been shown[6] that the NN Lu dipole occurs at approximately the same temperature as the NN Gd dipole, the A' peak has to be attributed to the relaxation of both defects, and the tetragonal paramagnetic center to the Gd NN dipole only. The subtraction of the concentration of NN dipoles as determined by EPR from the total concentration of dipoles estimated from the intensity of the ITC peak, gives the absolute concentration of NN Lu dipoles that is also represented in Fig. 9. The Lu NN dipole population is zero at very low Lu concentrations, then peaks

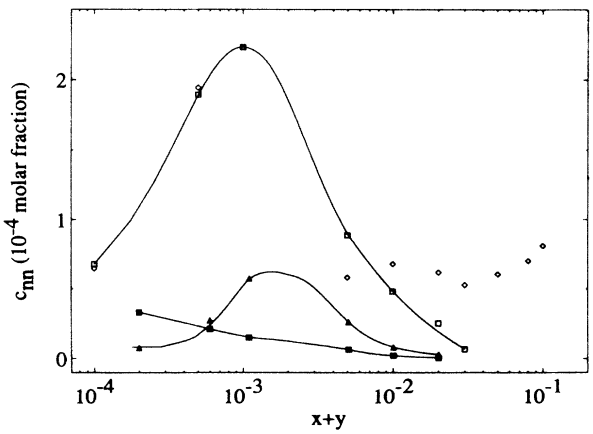

FIG. 9. Variation of the concentration of NN dipoles and tetragonal Gd^{3+} centers in the single- (open symbols) and double-doped (filled symbols) crystals as a function of the total rare-earth molar fraction, $x + y$. □: tetragonal Gd^{3+} centers as determined by EPR and ◇: NN Gd^{3+} dipoles as determined by ITC in $Ca_{1-x}Gd_xF_{2+x}$. ■: tetragonal Gd^{3+} centers as determined by EPR and ▲: NN Lu^{3+} dipoles as determined by ITC in $Ca_{1-x-y}Lu_xGd_yF_{2+x+y}$. The lines are drawn to guide the eye.

at $x \approx 2 \times 10^{-3}$; as compared to the concentration of NN Gd dipoles in the single-doped crystals, it is always much lower in the whole concentration range. This double origin for the A' peak explains its slight shift to lower temperatures as x increases and the Lu NN dipoles start outnumbering the Gd ones.

From Fig. 9 it is clear that the existence of NN dipoles in CaF_2 depends strongly on the rare-earth ion; intermediate size ions such as Gd^{3+} tend to be more stable in the first-neighbor position to their charge compensating defect than smaller trivalent ions. To explain the smaller amount of tetragonal centers either of Gd or Lu as compared to their abundance in the single-doped crystals, one could assume that the Lu^{3+} is either in cubic sites, free from the accompanying F_i^-, or in larger aggregates. The first assumption is consistent with a reduction in the number of Lu NN dipoles as compared to the single-doped material, but it does not explain the measured concentration of the Gd^{3+} NN dipoles that are less abundant in the double-doped crystals than in the single doped for x=0.0001. Moreover, the concentration of cubic Gd^{3+} centers is zero at this doping level in the double-doped crystal. The absence of Gd^{3+} either in cubic centers or in polarizable clusters and its low concentration in NN dipoles, as well as the nonexistence of Lu in NN dipoles indicates that even at this low x value the trivalent ions must be forming mixed clusters of larger size. Thus, the existence of high concentrations of Lu^{3+} ions in cubic sites that would not be detected either by ITC or EPR experiments is discarded and the missing Lu and Gd ions are assumed to be grouped in defect structures of higher complexity.

B. Cubic centers

The determination of the absolute concentration of the tetragonal centers by comparison with the number of NN dipoles as calculated from the ITC results, allows a calculation of the absolute concentration of the cubic Gd^{3+}, once the intensities have been normalized to the same experimental conditions (sample masses and theoretical intensity for both spectra). There are differences in the variation of the absolute concentrations of cubic Gd^{3+} in the single- and double-doped crystals which can be appreciated in Fig. 10. They are a strong indication of the dissimilarity in the clustering processes occurring in these two systems. In the $Ca_{1-x}Gd_xF_{2+x}$ solid solutions the cubic site concentration increases steeply with x, while the tetragonal to cubic site ratio decreases continuously for $x \geq 0.0001$. This behavior disagrees with the predictions of simple equilibrium models whereas as the number of free F_i^- increases the ratio of tetragonal to cubic site should also grow. If we assume that at the doping levels studied in this work the intrinsic defect equilibrium is negligible, the decrease of the concentration of any of the defects involved cannot be accounted for when the value of x increases.

An explanation currently accepted to account for these anomalies is to assume the existence of a scavenging process of fluoride interstitials by the other species coexisting in the crystal. These highly mobile interstitials

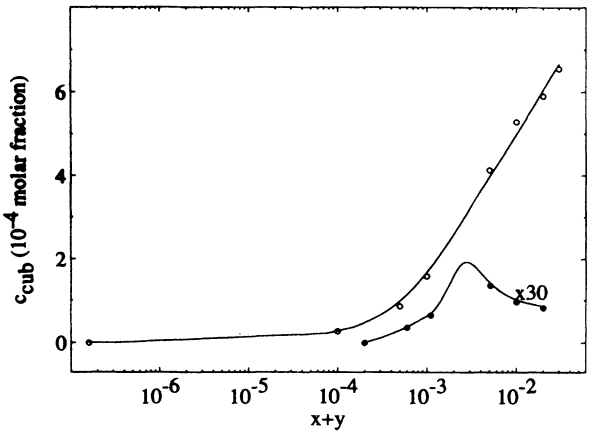

FIG. 10. Variation of the concentration of the cubic Gd^{3+} centers as a function of the total rare-earth molar fraction, $x+y$. ○: in $Ca_{1-x}Gd_xF_{2+x}$; ●: in $Ca_{1-x-y}Lu_xGd_yF_{2+x+y}$. The lines are drawn to guide the eye.

trapped in the vicinity of aggregates will not be able to form the number of NN dipoles required by the simple equilibrium laws, and the number of cubic centers will thus increase. Moreover, the cubic site concentration is strongly related to the total number of gettered aggregates. The relative stability of these clusters with extra interstitials has been estimated by using the standard computer simulation procedure as programmed in the HADES code by Corish *et al.*[2] and Bendall *et al.*[3] These authors have found that in the case of CaF_2:Gd^{3+} the energy changes on adding a free interstitial fluoride ion to NN or dimer complexes indicate a greater stability for the gettered cluster. Moreover, the abundance of cubic Gd^{3+} centers is consistent with the ITC results obtained on these same samples even if this technique is only sensitive to the dipolar defects. The variety of relaxation processes found in the single-doped matrix is the result of at least nine different dipolar species. The intensity variations of seven of these relaxations vs x are reported in Fig. 2. The gettered clusters have a dipolar moment and their reorientation in an electric field is possible and easy. Consequently, one can assert that the abundance of cubic sites as detected by EPR is a result of the existence of higher-order clusters that are further stabilized by the trapping of extra F_i^-. This trapping occurs during the cooling following the crystal growth at a temperature where the distribution of the clusters is already fixed by the small diffusion coefficient of the trivalent cations but is still sufficiently high for the F_i^- to be mobile and accommodate in the vicinity of the aggregates. Cirillo-Penn and Wright[22] have used a range of different kinetic models to fit their site selective laser spectroscopy results in CaF_2 doped with Eu^{3+}. They have found that only the model that assumes the existence of cubic, NN dipoles, gettered dimers, and gettered trimers was in agreement with their observations. In our Gd single-doped crystals the situation must be very similar except for the higher number of relaxations found by ITC that could be due to a greater number of polarizable clusters or to a va-

riety of relative positions of the extra F_i^- that slightly changes the relaxation times involved. Also, the result of the variation of the EPR linewidth vs x agrees with this interpretation. Both the cubic and the tetragonal spectrum show a progressive line broadening due to the dipolar interaction among the Gd^{3+} ions. This excludes the existence of very large aggregates that will concentrate most of the Gd and whose effect on these simple centers will be less intense.

The interpretation of the measured concentration of Gd cubic sites in the solid solutions $Ca_{1-x-y}Lu_xGd_yF_{2+x+y}$ cannot be made on the same assumptions as those valid for the Gd^{3+} and Eu^{3+} doped CaF_2. First, the double-doped matrix did not show the presence of abundant polarizable clusters in the temperature range explored here even for x values as high as 2%. Besides the peak originated by both the Gd^{3+} and the Lu^{3+} dipoles, there are only two very weak relaxations whose intensity does not grow with x but peaks at $x \simeq 0.002$. Second, even if we have no experimental evidence of a high number of cubic Lu^{3+} sites vs x, the discussion in the preceding section seems to discard it. Third, the number of NN dipoles detected is about an order of magnitude less than that observed for the single-doped matrix. Fourth, previous dielectric relaxation results down to liquid helium temperature[6] show the presence of an R_{III} relaxation around 20 K only for small radius impurities. This relaxation has been attributed to the reorientation of a high-order cluster, which seems reasonable in view of the energies involved at such low temperatures. These large clusters should contain several F_i^- and vacancies making the dipolar reorientation easy in the presence of an external field. Bevan[1] has proposed the existence of a long-range superstructure in the highly doped CaF_2:Y^{3+} in order to explain the x-ray diffraction patterns. These aggregates are hexamers that could be described as a cubo-octahedra composed of six trivalent cations, six F_i^- , and eight F^- relaxed from their normal positions, thus leaving the corners of the central cube of the defect unoccupied. However, this 6 | 0 | 8 | 6 in Bendall *et al.*[3] notation has a zero dipolar moment and cannot be the cluster responsible for the very low temperature relaxation observed by Andeen *et al.*[6] for the Lu^{3+} doped crystals at molar concentrations as low as 0.1%. Cirillo-Penn and Wright[22] recently proposed for the heavier rare earths, the existence of a more enriched F_i^- hexamer structure than that assumed previously. This extra F_i^- will destroy the high symmetry crystal field felt by the paramagnetic ions in the original 6 | 0 | 8 | 6 and consequently the EPR signal given by the Gd^{3+} ions in these clusters will be broad and weak.

The existence of different types of hexamers in our double-doped crystals at trivalent impurity levels as low as 0.0002 would explain several of our results. If for the very low x values the aggregates formed are the positively charged (deficient in F_i^-) 6 | 0 | 8 | 4_1 or 6 | 0 | 8 | 5_1, they would create an enrichment of F_i^- in the crystal with the corresponding reduction in the cubic Gd^{3+} sites. In fact, at low x values there do not exist any cubic Gd^{3+} centers. As x increases, only a very small amount of the Lu^{3+} ions is forming NN dipoles while the cubic Gd^{3+} sites increase; this indicates that the hexamers are trapping the F_i^- necessary to reach the 6 | 0 | 8 | 6 structure. The observed decrease in the intensity of the Gd^{3+} cubic and tetragonal spectra for $x > 0.001$ can be interpreted as due to the effective formation of Lu^{3+}+Gd^{3+} mixed clusters.

Another evidence for the existence of these large clusters in the double-doped crystals is the observation of a constant width for the EPR lines due to the tetragonal, or even a reduction in the case of the cubic Gd^{3+} spectra as the Lu^{3+} concentration increases as can be observed in Fig. 8. If the zero-spin Lu^{3+} ions were in the form of monomers or small nonpolarizable clusters, they will cause heterogeneities in the crystal field felt by the paramagnetic ions, resulting in a line broadening which will increase with x as they will depend on the distance of these clusters from the paramagnetic probes. If the Lu^{3+} ions are grouped from very low concentrations in very large aggregates like the hexamers, the effect on the crystalline field felt by the Gd^{3+} ions in constant concentration will be very small as the distances involved will be quite large.

C. Larger clusters

As no evidence of the existence of oxygen compensation has been found in our samples, as could have been the T_1 or T_2 centers easily detected by EPR when the samples were thermally treated, the following discussion will be based on F_i^- compensation. In $Ca_{1-x}Gd_xF_{2+x}$ eight peaks have been attributed to polarizable clusters made by more than two point defects. The NNN dipole has been discarded as no paramagnetic center with trigonal symmetry was ever detected. The HADES simulations[1,2] have shown an increased stability as the clusters scavenge an extra fluorine ion from the other complexes existing in the lattice. It is the only way for these complexes to become polarizable and the variety of relaxations found here clearly demonstrates that this trapping process is indeed occurring in the CaF_2:Gd^{3+} system.

In the $Ca_{1-x-y}Lu_xGd_yF_{2+x+y}$ the coexisting clusters are found to be radically different from those discussed above. First, we found no evidence of polarizable complexes increasing in number with the Lu concentration from 77 to 350 K. Only at temperatures around 20 K a dielectric relaxation peak was observed[6] for the small impurities starting from Tb. As stated above the variation of the concentration of simple defects is consistent with the formation of different types of hexamers that would be stable from very low concentrations. The results of the HADES calculation do not predict these differences as the calculated stability of the various hexamers are not very different in the case of Gd or Lu. From their results Y^{3+} is the cation that definitely shows an increased lattice stability upon hexamer formation. Lu^{3+} and Gd^{3+} do not show significant differences. The small differences observed on the energy changes on forming hexamer complexes from dimer clustering indicate, however, a greater stability in the case of the Lu^{3+} doped CaF_2. The ex-

tended x-ray-absorption fine structure (EXAFS) results obtained by Catlow *et al.*[23] on highly doped ($x = 10\%$) CaF_2 with several trivalent cations show that at this concentration the predominant cluster is the same from Gd to Yb and of another type for La, Pr, and Nd. The EXAFS patterns support the idea of a transition from small dimeric clusters to hexamers on going from Nd to Er. Moreover, for this last cation they have shown that the hexamer maintains its structure in the temperature range 298–1070 K. Our results indicate that in the Gd^{3+} doped crystals the nucleation of the large clusters, which is taking place in the concentration range under study, still results from the aggregation of intermediate size aggregates while in the case of the Lu hexamers they already exist at very low concentrations. The similar results obtained with the HADES program could be due to the use of the same reaction for the clustering process that instead seems to be very different. It is to be noted that the ionic radius of the Lu^{3+} ion in an eight-coordination site is the smallest of the trivalent cations,[24] i.e., 1.11 Å. If the cationic size is the relevant factor in determining the clustering processes, Lu^{3+} should be similar to Y^{3+}, whose ionic radius is 1.155 Å. Another evidence for the existence of these large clusters only in the double-doped crystals, even at very low concentrations, is the presence of mechanical strains that could be observed during the sample cleavage and did not exist in the single-doped ones.

V. CONCLUSIONS

The comparative studies carried on in this work on Gd single-doped and Gd+Lu double-doped CaF_2 crystals by ITC and EPR techniques have completed the picture of the coexistence of different size defects in fluorites. Strong differences have been found among the two types of solid solutions. In the single-doped crystals we have found an extremely rich ITC spectrum with at least nine different relaxations in the temperature range explored. These results are very much in line with those obtained with site selective laser spectroscopy[22] on CaF_2:Eu^{3+} where the dimers and trimers dominate the clustering of the large trivalent cations. The ITC technique offers the advantage of being able to differentiate among species with the same number of cationic impurities but with a slight different distribution in the extra F_i^-. Moreover, we also agree with the results obtained by using the HADES simulations and the increased stability reached by the trapping of extra F_i^-. However, the number of different relaxation times found here indicates that more models have to be considered in order to account for the observed number of different aggregates. The EXAFS pattern interpretation of heavily doped crystals, which suggests that on starting from Gd the clustering is based on cubo-octahedra, is a much more indirect evidence than the one gathered here and by laser spectroscopy.

The fundamental differences found here on the double-doped matrix with Gd and Lu CaF_2 crystals as compared to the single-doped matrix, have shown that the clustering processes at this intermediate concentration range cannot be interpreted as the scavenging of F_i^- by various clusters of increasing size. Here the existence of the cubo-octahedra aggregates even at low impurity concentrations is the only explanation that takes into account the observed abundance variation of the cubic and tetragonal centers, as well as the variation of the EPR linewidths vs x. The HADES simulations predict clearly this kind of aggregates for CaF_2:Y^{3+}. Lu^{3+}, which is still smaller than Y^{3+}, must follow the same behavior and the differences obtained in the stabilities calculation must be due to the noninclusion of the lattice distortions and strain interactions that are certainly present in this system.

ACKNOWLEDGMENTS

This research was supported in part by the Consejo Nacional de Investigaciones Científicas y Tecnológicas (CONICIT S1-1422).

[1] D. J. M. Bevan, J. Strahle, and O. Greis, J. Solid State Chem. **44**, 75 (1982).
[2] J. Corish, C. R. A. Catlow, P. W. M. Jacobs, and S. H. Ong, Phys. Rev. B **25**, 6425 (1982).
[3] P. J. Bendall, C. R. A. Catlow, J. Corish, and P. W. M. Jacobs, J. Solid State Chem. **51**, 159 (1984).
[4] R. Capelletti, E. Okuno, G. E. Matthews, and J. H. Crawford, Jr., Phys. Status Solidi A **47**, 617 (1978).
[5] D. R. Figueroa, E. Laredo, M. Puma, and N. Suarez, Cryst. Lattice Defects **9**, 167 (1982).
[6] C. A. Andeen, J. J. Fontanella, M. C. Wintersgill, P. J. Welcher, R. J. Kimble, and G. E. Matthews, J. Phys. C **14**, 3557 (1981).
[7] E. Friedman and W. Low, J. Chem. Phys. **33**, 1275 (1960).
[8] Chi-Chung Yang, Sook Lee, and Albert J. Bevolo, Phys. Rev. B **12**, 4687 (1975).
[9] Chi-Chung Yang, Sook Lee, and Albert J. Bevolo, Phys. Rev. B **13**, 2762 (1976).
[10] F. Z. Gil'fanov, L. D. Livanova, and A. L. Stolov, Fiz. Tverd. Tela (Leningrad) **8**, 142 (1966) [Sov. Phys. Solid State **8**, 108 (1966)].
[11] R. H. Petit, P. Evesque, and J. Duran, J. Phys. C **14**, 5081 (1981).
[12] A. Lezama, M. Oriá, and C. B. Araujo, Phys. Rev. B **33**, 4493 (1986).
[13] D. R. Tallant and J. C. Wright, J. Chem. Phys. **63**, 2074 (1975).
[14] D. R. Tallant, D. S. Moore, and J. C. Wright, J. Chem. Phys. **87**, 2897 (1977).
[15] D. S. Moore and J. C. Wright, J. Chem. Phys. **74**, 1626 (1981).
[16] E. Secemski and W. Low, J. Chem. Phys. **64**, 4240 (1976).
[17] J. M. O'Hare, J. Chem. Phys. **57**, 3838 (1972).
[18] E. Laredo, M. Puma, and D. R. Figueroa, Phys. Rev. B **19**, 2224 (1979).
[19] E. Laredo, M. Puma, N. Suarez, and D. R. Figueroa, Phys.

Rev. B **23**, 3009 (1981).
[20]M. Puma, E. Laredo, A. Bello, M. E. Galavis, and N. Suarez, J. Phys. C **21**, 5555 (1988).
[21]M. Díaz, M. Puma, E. Laredo, A. Bello, and N. Suarez, J. Phys.: Condens. Matter **2**, 9879 (1990).
[22]K. M. Cirillo-Penn and J. C. Wright, Phys. Rev. B **41**, 10799 (1990).
[23]C. R. A. Catlow, A. V. Chadwick, G. N. Greaves, and L. M. Moroney, Cryst. Lattice Defects Amorph. Mater. **12**, 193 (1985); C. R. A. Catlow, A. V. Chadwick, J. Corish, L. M. Moroney, and A. N. O'Reilly, Phys. Rev. B **39**, 1897 (1989).
[24]R. D. Shannon and C. T. Prewitt, Acta Crystallogr. B **25**, 925 (1969).